

Homonuclear decoupling for enhancing resolution and sensitivity in NOE and RDC measurements of peptides and proteins



Jinfa Ying, Julien Roche, Ad Bax*

Laboratory of Chemical Physics, National Institute of Diabetes and Digestive and Kidney Diseases, National Institutes of Health, Bethesda, MD 20892, USA

ARTICLE INFO

Article history:

Received 14 October 2013

Revised 11 November 2013

Available online 22 November 2013

Keywords:

Diffusion anisotropy

IDP

Residual dipolar coupling

RDC

Weak alignment

Liquid crystal

NOESY

Synuclein

Ubiquitin

ABSTRACT

Application of band-selective homonuclear (BASH) ^1H decoupling pulses during acquisition of the ^1H free induction decay is shown to be an efficient procedure for removal of scalar and residual dipolar couplings between amide and aliphatic protons. BASH decoupling can be applied in both dimensions of a homonuclear 2D NMR experiment and is particularly useful for enhancing spectral resolution in the $\text{H}^{\text{N}}-\text{H}^{\alpha}$ region of NOESY spectra of peptides and proteins, which contain important information on the backbone torsion angles. The method then also prevents generation of zero quantum and $\text{H}_z^{\text{N}}-\text{H}_z^{\alpha}$ terms, thereby facilitating analysis of intraresidue interactions. Application to the NOESY spectrum of a hexapeptide fragment of the intrinsically disordered protein α -synuclein highlights the considerable diffusion anisotropy present in linear peptides. Removal of residual dipolar couplings between H^{N} and aliphatic protons in weakly aligned proteins increases resolution in the $^1\text{H}-^{15}\text{N}$ HSQC region of the spectrum and allows measurement of RDCs in samples that are relatively strongly aligned. The approach is demonstrated for measurement of RDCs in protonated $^{15}\text{N}/^{13}\text{C}$ -enriched ubiquitin, aligned in Pf1, yielding improved fitting to the ubiquitin structure.

Published by Elsevier Inc.

1. Introduction

It has long been recognized that removal of homonuclear $^1\text{H}-^1\text{H}$ or $^{13}\text{C}-^{13}\text{C}$ J couplings can significantly improve spectral resolution of 2D NMR spectra. In the indirectly detected t_1 dimension, this typically has been done either by using constant-time evolution [1–3] or, in the case of heteronuclear experiments, by application of a single BIRD pulse unit [4]. Alternatively, a combination of a non-selective 180° pulse and a frequency-selective pulse applied during a static gradient can be used to obtain broad-band $^1\text{H}-^1\text{H}$ decoupling [5–7]. This latter method, referred to as Zangger-Sterk or ZS, utilizes the non-selective/selective 180° pulse pair to invert all protons outside of the region inverted by the selective pulse [8]. Inside the selective-pulse-inverted region, the net rotation of the non-selective and selective 180° pulses is zero, and no net evolution of chemical shift or J couplings occurs during the selective pulse and its associated pulsed field gradients. The elegant ZS method is very effective at eliminating $^1\text{H}-^1\text{H}$ J couplings in a broad-band fashion, although the number of observed spins and thereby the intrinsic sensitivity of the experiment decreases in proportion to the thickness of the sample slice selected by the ZS pulse combination.

In the directly detected dimension, removal of the $^1\text{H}-^1\text{H}$ J couplings also can be achieved by bilinear rotation decoupling (BIRD), which relies on periodically inverting all ^1H spins that are not directly attached to ^{13}C [9], but limits detection to protons attached to ^{13}C , the latter being either at natural abundance or low levels of random enrichment. As was demonstrated very recently, ZS pulse/gradient combinations can also be applied during an interrupted FID, which then accomplishes homonuclear broad-band decoupling in the directly detected dimension [6]. This particularly elegant method results in dramatic spectral simplification, but again involves a significant cost in sensitivity related to slice selection. In favorable cases, the sensitivity loss can be minimized, however, by rapidly repeating the experiment on adjacent, non-perturbed regions of the sample [7].

For peptides and proteins, frequently much of the interest is focused on detection of amide protons. This includes the widely used $^1\text{H}-^{15}\text{N}$ HSQC experiment [10,11], and the large battery of amide-detected triple resonance experiments [12–14]. In particular when using protein samples in a weakly aligned state, necessary for the measurement of residual dipolar couplings, the presence of $^1\text{H}^{\text{N}}-^1\text{H}^{\alpha}$ as well as other $^1\text{H}^{\text{N}}-^1\text{H}^{\text{sidechain}}$ residual dipolar couplings can significantly limit the spectral resolution and sensitivity. As demonstrated by Vander Kooi et al. [15], band-selective decoupling of the aliphatic proton region can relieve this problem, and can be accomplished by alternately gating the ^1H homonuclear transmit channel and the ^1H receiver to periodically invert the aliphatic

* Corresponding author. Fax: +1 301 402 0907.

E-mail address: bax@nih.gov (A. Bax).

protons during acquisition of the FID. Analogous removal of ${}^3J_{\text{HH}}$ splittings in NOESY spectra by applying G3-shaped pulses through the homonuclear decoupling channel has been demonstrated by Hammerström and Otting [16]. Technically these methods are challenging, in part due to the difficulty in suppression of the water signal, and also due to the introduction of time-dependent Bloch–Siegert shifts caused by the decoupling RF irradiation. As a result, these methods have not yet become widely used.

Here, we describe an alternate method to achieve band-selective homonuclear (BASH) decoupling in peptides and proteins, using an approach that is essentially a hybrid of the Zangger–Sterk and Hammerström methods. BASH is particularly effective for gaining increased spectral resolution in 2D $\text{H}^{\text{N}}\text{--}\text{H}^{\alpha}$ NOE spectra, and then has the additional advantage of eliminating the generation of multi-quantum and zz spin states during the mixing period, which can adversely affect spectral quality. Much recent interest focuses on intrinsically unstructured proteins, where the spectral dispersion in both H^{N} and H^{α} regions is poor, and the additional resolution gained by homonuclear decoupling then is particularly valuable. Considerable variation in the ratio of the intraresidue over the sequential $\text{H}^{\text{N}}\text{--}\text{H}^{\alpha}$ NOE was recently reported for the intrinsically disordered protein α -synuclein [17]. This NOE ratio can be a sensitive reporter for the backbone torsion angle ψ , which is difficult to evaluate by alternate methods [18].

A weakly ordered aqueous environment is commonly used for measurement of residual dipolar couplings (RDCs) in proteins [19]. The filamentous phage Pf1 is particularly widely used for this purpose as it is highly stable and commercially available [20]. Due to its large negative surface charge of ca 0.5 e/nm², some proteins align particularly strongly in this medium. It then can be challenging to generate conditions where the Pf1 remains liquid crystalline while the protein is aligned sufficiently weakly that homonuclear ${}^1\text{H}\text{--}{}^1\text{H}$ couplings do not dramatically decrease resolution and sensitivity of the ${}^1\text{H}\text{--}{}^{15}\text{N}$ HSQC spectrum. For example, for recording spectra on the widely studied protein ubiquitin, alignment in Pf1 tends to be quite strong, making it necessary to increase ionic strength to decrease protein alignment. This increased ionic strength, in turn, can lead to a paranematic phase or phase separation of the Pf1 [21]. As previously demonstrated by Vander Kooi et al. [15], homonuclear decoupling is an effective solution to remove the ${}^1\text{H}\text{--}{}^1\text{H}$ RDCs and thereby increase spectral resolution. We here demonstrate the BASH decoupling method for this purpose.

2. Results and discussion

2.1. The basic BASH scheme

The pulse sequence for recording the one-dimensional BASH-decoupled amide ${}^1\text{H}$ spectrum of a peptide or protein is shown in Fig. 1. Because selective and non-selective radiofrequency (RF) ${}^1\text{H}$ pulses are applied during the FID, and the spectra necessarily are recorded on samples dissolved in H_2O , adequate suppression of the intense water signal is important. To this extent, we find it necessary in homonuclear ${}^1\text{H}$ experiments to include weak (~ 25 Hz RF field) presaturation of the water resonance, in addition to using an excitation scheme that does not excite any residual water magnetization. In Fig. 1, we use the $90_x\text{--}\tau\text{--}90_{-x}$ jump-and-return sequence [22] for this purpose, or alternatively an EBURP pulse [23] can be used. This excitation is followed by an amide ${}^1\text{H}$ band-selective REBURP pulse [23], surrounded by gradients (G_2), to further suppress the water signal. The actual BASH decoupling is achieved by inserting a combination of a band-selective 180°_x together with a non-selective 180°_x pulse, which flips the spin state of all protons outside of the selected amide band [8]. It is important

that the two pulses have the exact same phase (or the exact opposite phase), as otherwise a jump in the phase of the transverse magnetization would occur each time this pulse combination is applied. Net evolution of the amide ${}^1\text{H}$ transverse magnetization is zero over the total interval used for application of the two pulses and the short gradient pulses surrounding each ${}^1\text{H}$ pulse. In order to minimize refocusing of water magnetization, excited by imperfection of e.g. the first 180° pulse pair, that will occur if a second subsequent gradient pulse pair is applied that uses the same set of pulsed field gradients, we use different gradient strengths for the second pulse pair. In principle it would be advantageous to ensure that all subsequent 180° pulse pairs are surrounded by gradients that differ from those applied previously, but in practice the occurrence of such echoes is difficult to suppress completely and we find that simply repeating this “double block” of (acquire T , pp1, acquire $2T$, pp2, acquire T) suffices. Here, pp1 and pp2 refer to the first and second set of pulse pairs with associated gradient pulses, and $2T$ is the separation between the pulse pairs. Similarly to the X,X,-X,-X phase alternation used in heteronuclear decoupling schemes such as MLEV4 [24], phases of two consecutive 180° pulse pairs, within the bracketed loop, are inverted each time the loop is repeated.

As discussed by Aguilar et al. [25] and Meyer and Zangger [6], it is important to keep the duration of $2T$ much smaller than $1/J_{\text{HH}}$. If not, decoupling sidebands in the spectrum will occur at distances of $(4T)^{-1}$ from the decoupled resonances. These sidebands can become more significant if an antiphase term of the type $2\text{H}_x^{\text{N}}\text{H}_z^{\alpha}$ is present prior to application of the pulse train of Fig. 1A, and then appear as an antiphase doublet with a splitting of $(2T)^{-1}$, centered around the resonance of interest. In the limit where $J_{\text{HH}} \ll (2T)^{-1}$, the intensity of the antiphase decoupling sidebands approximately scales with $2T * J_{\text{HH}}$, whereas the amplitudes of the in-phase decoupling sidebands scale with $(2T * J_{\text{HH}})^2$, therefore presenting less of a problem.

The line width of the decoupled resonance is increased somewhat relative to its natural T_2 -limited value for two reasons: First, relaxation losses during the pulse pair increase the apparent decay rate by a factor $(2T + \text{pp})/(2T)$, where pp is the duration of the pulse pair and its associated pulsed field gradients. Second, pulse imperfections in the 180° pulses result in a loss of magnetization each time such a pair is applied. If a fraction, α , of the magnetization is returned to its position immediately preceding that pulse pair, the apparent additional contribution to the decay rate equals $-\ln(\alpha)/2T$. Both relaxation losses and losses due to pulse imperfections are minimized when $2T$ is kept large, and this requirement therefore competes with the desire to keep the sidebands small. For random coil peptides, where ${}^3J_{\text{HN--H}\alpha} \approx 7$ Hz, we find a $2T$ duration of $\sim 10\text{--}25$ ms to be a reasonable compromise between these separate requirements.

Fig. 2A/B compares the BASH spectrum of the amide region of the N-terminal acetylated, C-terminally amidated hexapeptide Ac-VAAAEK-NH₂ with the corresponding regular 1D spectrum. The spectrum, recorded at 747 MHz ${}^1\text{H}$ frequency, shows a clear collapse of the doublets, with only a modest, <1 Hz, increase in line width in the decoupled spectrum relative to the reference spectrum. The two spectra are displayed at the same scaling relative to the thermal noise, indicating an increase in true signal to thermal noise ratio upon BASH decoupling. However, small decoupling sidebands in the BASH spectrum (Fig. 2B) decrease the apparent S/N in this spectrum.

2.2. BASH-decoupled NOESY

Removal of ${}^3J_{\text{HH}}$ couplings is particularly useful when analyzing 2D (or 3D) NOESY spectra of peptides or intrinsically disordered proteins (IDPs). Whereas ${}^3J_{\text{HH}}$ provides an accurate constraint for

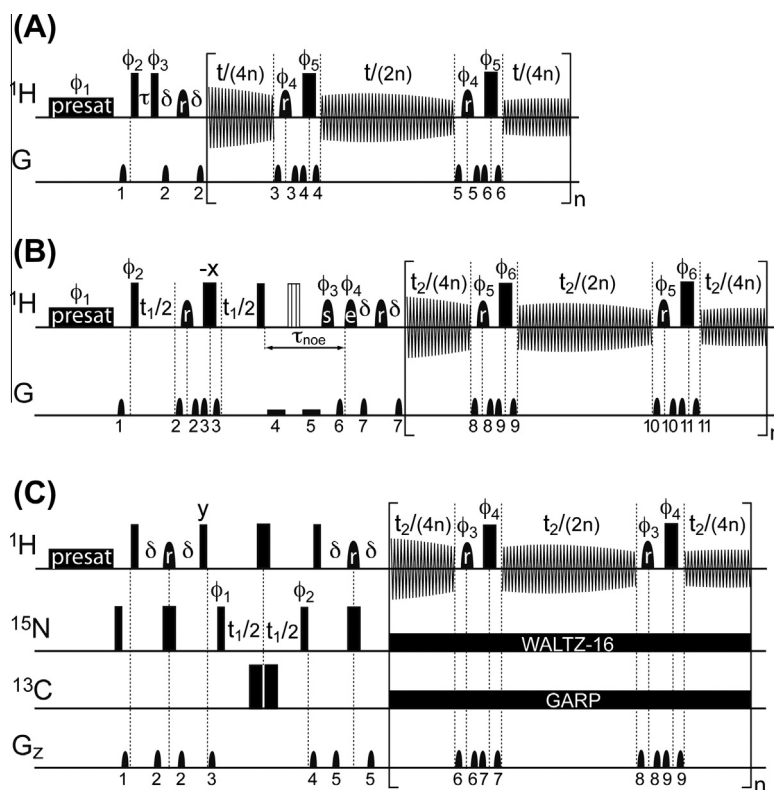


Fig. 1. Pulse sequences using band-selective homonuclear decoupling during data acquisition. (A) Pulse scheme for recording a 1D spectrum of the amide region of peptides and proteins, with BASH decoupling of aliphatic protons. (B) 2D NOESY pulse scheme, with BASH decoupling during both t_1 evolution and t_2 detection periods. The BASH decoupling during t_1 evolution only requires a single pulse pair, with the band-selective pulse applied to the H^α region, and decouples it from $^1H^\beta$ and $^1H^N$ protons. Decoupling in this dimension will not remove geminal $^1H^{\alpha 2}-^1H^{\alpha 3}$ J couplings in Gly, nor $^1H^{\alpha}-^1H^\beta$ J couplings in Thr and Ser residues, as these typically resonate in the same spectral region as the $^1H^\alpha$ protons selected by the BASH pulse. (C) Pulse scheme for the $^1H-^{15}N$ 2D HSQC spectrum with BASH decoupling during t_2 . Shaped pulses marked r are REBURP 180° pulses [23] (1.6 ms centered at 9.67 ppm for the HSQC on Pf1-aligned ubiquitin at 500 MHz and 2 ms centered at 8.6 ppm for the 1D and 2D NOESY on the hexapeptide at 747 MHz). The shaped pulse marked s is a 1-ms (at 747 MHz) sinc-shaped selective $^1H^\alpha$ pulse, centered at 4.2 ppm. The shaped pulse marked e is an EBURP2 pulse [23], centered at 8.6 ppm, of duration 2.0 ms (747 MHz). H_2O presaturation is used (25 Hz RF field strength) during the delay between scans. Specific parameters for scheme (A): $t/4n = 12$ ms; $n = 9$; phase cycling: $\phi_1 = x, x, x, -x, -x$; $\phi_2 = -x, x$; $\phi_3 = x, -x$; $\phi_4 = -x$ and $\phi_5 = x$ for the odd blocks, and inverted for even numbered values of the loop counter, n ; Rec. = $x, -x$; delays: $\tau = 83$ μ s; $\delta = 2.2$ ms; gradient durations: $G_{1,2,3,4,5,6} = 1.2, 2, 0.3, 0.37, 0.3, 0.37$ ms; gradients are all sine bell shaped with maximum amplitude (x, y, z) $G_{1,2,3,4,5,6} = (25.2, 25.2, 35.7), (0, 0, 38.5), (18.3, 0, 0), (0, 18.3, 0), (16.3, 11.4, 1.4), (16.3, 1.5, 15.4)$ G/cm; Specific parameters for scheme (B): $t_2/4n = 12$ ms; $n = 6$; phase cycling: $\phi_1 = 8(x), 8(-x)$ $\phi_2 = x, x, x, -x, -x$; $\phi_3 = 4(x), 4(-x)$; $\phi_4 = -x, x$; $\phi_5 = -x$ and $\phi_6 = x$ for the odd-numbered values of the loop counter, n , and inverted for even values of n ; Rec. = $x, -x, -x, x, x$; delay: $\delta = 2.2$ ms; gradient durations: $G_{1,2,3,6,7,8,9,10,11} = 1.2, 0.37, 0.3, 5, 2, 0.3, 0.37, 0.3, 0.37$ ms; gradients 1–3 and 6–11 are all sine bell shaped with maximum amplitude (x, y, z) $G_{1,2,3,6,7,8,9,10,11} = (25.2, 25.2, 35.7), (18.3, 0, 0), (16.3, 11.4, 1.4), (15.3, 1.5, 15.4), (0, 0, 38.5), (18.3, 0, 0), (0, 18.3, 0), (16.3, 11.4, 1.4), (15.3, 1.5, 15.4)$ G/cm; gradients G_4 and G_5 are rectangular with amplitudes $G_{4,5} = (0.5, 0.5, 0.7)$ and $(-0.6, -0.6, -0.9)$ G/cm and durations slightly less than half the NOE mixing time, $\tau_{noe}/2$. The open pulse in the center of τ_{noe} represents a $90_2 210_0 90_x$ composite inversion pulse. Quadrature in the t_1 dimension is accomplished by State-TPPI phase incrementation of ϕ_2 . Specific parameters for scheme (C): $t_2/4n = 5$ ms; $n = 4$; phase cycling: $\phi_1 = x, -x$; $\phi_2 = x, x, x, -x, -x$; $\phi_3 = x$ and $\phi_4 = -x$ for the odd values of n and inverted for even values; Rec. = $x, -x, -x, x, x$; delays: $\delta = 1.9$ ms; gradient durations: $G_{1,2,3,4,5,6,7,8,9} = 1.7, 1.7, 1.1, 1.2, 1.4, 0.21, 0.21, 0.21, 0.21$ ms; gradients are all sine bell shaped with maximum amplitude $G_{1,2,3,4,5,6,7,8,9} = 35.7, 2.1, 28.7, 20.8, 32.9, 14.7, 21, 25.9, 32.9$ G/cm; Quadrature in the t_1 dimension is accomplished by State-TPPI phase incrementation of ϕ_1 . The pulse sequences and parameters for all three pulse schemes can be downloaded from <http://spin.niddk.nih.gov/bax/pp/>.

the time-averaged backbone torsion angle ϕ , experimental parameters that are impacted by the ψ angle, such as $^1J_{C^\alpha H^\alpha}$, $^1J_{C^\alpha N}$, and $^2J_{C^\alpha N}$ or the backbone $^{13}C^\alpha$ chemical shift are much less precise parameters for defining this backbone torsion angle [26]. Gagne et al. proposed to use the ratio of sequential to intrasidue $H^\alpha-H^N$ NOE intensities, $d_{\alpha N}(i-1, i)/d_{\alpha N}(i, i)$, for this purpose [18]. Provided that both types of interproton interactions are subject to the same spectral density function, this NOE ratio ranges from ca 0.25 in α -helical conformations ($\psi \approx -50^\circ$) to ca 4 for an extended conformation ($\psi \approx +120^\circ$). In intrinsically disordered proteins, this NOE ratio is typically found to be remarkably high, in the 3–6 range, suggesting that the backbone exclusively adopts extended conformations, in the β and polyproline II (PPII) region, which in turn conflicts with the presence of relatively intense sequential H^N-H^N NOEs [17]. By recording a BASH-NOESY spectrum on the above introduced hexapeptide, we here demonstrate that as a result of rotational diffusion anisotropy, the sequential and intrasidue $^1H^\alpha-^1H^N$ NOEs are subject to substantially different time

dependence of their auto-correlation function, even in relatively short peptides, an effect exacerbated in IDPs.

Fig. 2C/D compares the BASH 2D NOESY spectrum, recorded on Ac-VAAAEK-NH₂ with its regular 2D NOESY equivalent. The very weak NOEs (all smaller than $\pm 0.2\%$ relative to the diagonal) are dwarfed by zero quantum J -correlation contributions in the regular NOESY spectrum (Fig. 2C). By comparison, the BASH NOESY spectrum (Fig. 2D) not only suppresses these J -correlation contributions, but can be plotted at a lower contour level relative to the thermal noise because it has strongly reduced t_1 noise ridges. This suppression of t_1 noise is associated with the removal of the intense diagonal resonances by the BASH pulse pair and its accompanying pulsed field gradients applied at the midpoint of t_1 evolution. Additional suppression of t_1 noise is accomplished by the non-selective 180° 1H pulse, applied at the midpoint of the mixing period. This latter 180° 1H pulse prevents buildup of net H^N magnetization due to T_1 relaxation during the NOE mixing period, whose imperfect subtraction upon phase cycling of the 90_{ϕ_1} pulse also

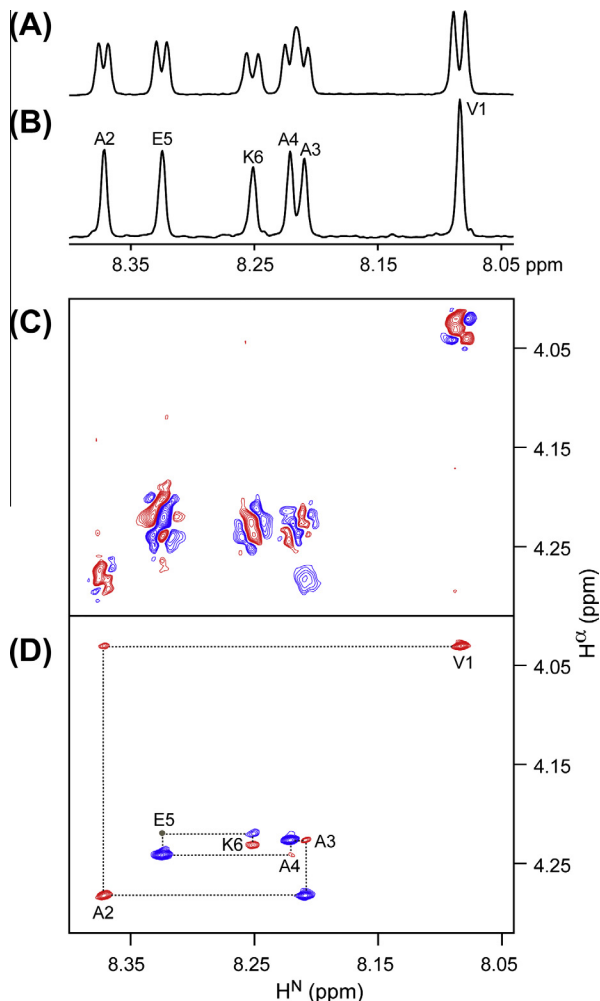


Fig. 2. Comparison of BASH-decoupled and regular ^1H spectra of a linear hexapeptide, Ac-VAAAEK-NH₂ (10 mM), recorded at 747 MHz ^1H frequency, 25 °C, pH 6.0, 20 mM sodium phosphate, with the pulse schemes of Fig. 1A and B. The peptide corresponds to residues 16–21 of α -synuclein. (A) Amide region of the regular ^1H spectrum, recorded with weak (25 Hz RF field) presaturation of the H₂O resonance. (B) BASH decoupled amide region. (C) $\text{H}^\alpha\text{-H}^{\text{N}}$ region of the regular 2D NOESY spectrum, recorded with a 200 ms NOE mixing time, using acquisition times of 133 ms (t_1) and 274 ms (t_2). NOEs for this peptide are very weak, due to the condition $\omega\tau_c \approx 1$, and cross peaks are dominated by coherent (zero quantum) contributions. The only NOE cross peak clearly visible is the sequential NOE from A2–H $^\alpha$ to A3–H $^{\text{N}}$ and corresponds to a cross relaxation rate of $-0.01 \pm 0.002 \text{ s}^{-1}$. Blue contours correspond to positive intensity (with the diagonal being positive); red depicts negative intensity. (D) $\text{H}^\alpha\text{-H}^{\text{N}}$ region of the 2D BASH-NOESY spectrum, recorded with the pulse scheme of Fig. 1B, using a 200 ms NOE mixing time and acquisition times of 319 ms (t_1) and 270 ms (t_2). Blue cross peaks correspond to $\omega\tau_c > 1$ and all are sequential $\text{H}^\alpha\text{-H}^{\text{N}}$ NOEs; red cross peaks have negative intensity, i.e. $\omega\tau_c < 1$, and with one exception (V1–A2) are all intrasidue and labeled by residue type and number. The absolute value of the intrasidue $\text{H}^\alpha\text{-H}^{\text{N}}$ NOE of E5 falls below the detection threshold ($\sigma < 10^{-3} \text{ s}^{-1}$).

would contribute to t_1 noise. A disadvantage of the BASH NOESY method is that a separate spectrum needs to be recorded to obtain diagonal intensities, which can be accomplished by simply shifting the band-selective ^1H 180° pulse at the midpoint of t_1 from the H^α to the H^{N} region. Such a diagonal reference spectrum, which has very high signal to noise, can be recorded rapidly with very few scans and increments, followed by rescaling the diagonal intensities to those applicable for the conditions used to measure the $\text{H}^\alpha\text{-H}^{\text{N}}$ 2D BASH NOESY spectrum. The weakest cross peak observed in the spectrum of Fig. 2D is for the intrasidue $\text{H}^\alpha\text{-H}^{\text{N}}$ interaction of residue A4, corresponding to 0.04%, or a cross relax-

ation rate σ of 0.002 s^{-1} . The only missing cross peak is for the intrasidue $\text{H}^\alpha\text{-H}^{\text{N}}$ interaction of residue E5, which falls below the detection threshold of 0.02%.

Assuming a prolate ellipsoid shape, with rotational diffusion constants D_{\parallel} and D_{\perp} around its long and short axes, the rotational correlation time, $\tau_c = 1/(2D_{\parallel} + 4D_{\perp})$, for this peptide falls close to the condition where NOEs are zero, i.e. $\omega_{\text{H}}\tau_c \approx 1.1$. Interestingly, at this magnetic field strength (747 MHz ^1H frequency) and temperature (298 K), the sequential NOEs are negative for all but the terminal V1–A2 interaction, whereas all intrasidue $\text{H}^\alpha\text{-H}^{\text{N}}$ NOEs are weak and positive, highlighting the faster decay of the auto-correlation function for the intrasidue $\text{H}^\alpha\text{-H}^{\text{N}}$ interactions compared to the sequential ones. Considering that the intrasidue $\text{H}^\alpha\text{-H}^{\text{N}}$ distance falls in the 2.7–3 Å range in the populated negative ϕ region of Ramachandran space, the positive signs of the intrasidue $\text{H}^\alpha\text{-H}^{\text{N}}$ cross relaxation rates as well as the terminal sequential V1–A2 NOE reflect the shorter effective correlation times for these interactions compared to the oppositely signed sequential $\text{H}^\alpha\text{-H}^{\text{N}}$ NOEs. In the allowed region of Ramachandran space, intrasidue $\text{H}_i^\alpha\text{-H}_i^{\text{N}}$ vectors are at angles larger than 45° relative to the $\text{C}_{i-1}^\alpha\text{-C}_i^\alpha$ chain direction whereas sequential $\text{H}_{i-1}^\alpha\text{-H}_i^{\text{N}}$ vector are approximately parallel to the $\text{C}_{i-1}^\alpha\text{-C}_i^\alpha$ chain direction when ψ is in the extended range ($\psi = 120 \pm 60^\circ$), where the $\text{H}_{i-1}^\alpha\text{-H}_i^{\text{N}}$ distance is shortest. The opposite signs for the intrasidue and sequential $\text{H}^\alpha\text{-H}^{\text{N}}$ NOE therefore reflect considerable anisotropy of the peptides rotational diffusion tensor. This variation in applicable spectral density is confirmed by recording the BASH-NOESY spectra at different magnetic field strengths and temperatures (data not shown).

2.3. BASH-decoupled HSQC

When aligning fully protonated ^{15}N - or $^{15}\text{N}/^{13}\text{C}$ -enriched proteins in a liquid crystalline medium, in order to measure residual heteronuclear dipolar couplings, residual $^1\text{H}\text{-}^1\text{H}$ dipolar couplings can adversely impact the achievable resolution and sensitivity of such spectra. Pulse schemes used for measuring RDCs are mostly of the 2D $^1\text{H}\text{-}^{15}\text{N}$ HSQC or HSQC-TROSY type [27–29], or 3D triple resonance extensions that include such $^1\text{H}\text{-}^{15}\text{N}$ HSQC or TROSY-HSQC pulse sequence element [30]. For a number of liquid crystalline media, it can be challenging to reach a degree of protein alignment that is sufficiently weak for facile measurement of the RDCs. For example, measurements of $^1\text{H}\text{-}^{15}\text{N}$ RDCs in ubiquitin aligned in a liquid crystalline Pf1 suspension requires conditions where the nematogen is close to the edge of its liquid crystalline phase diagram, in order to reduce $^1D_{\text{NH}}$ couplings to values less than ca ± 30 Hz. Under these conditions, $^1\text{H}\text{-}^1\text{H}$ RDCs can approach similarly large values. The simultaneous presence of both large and small $^1\text{H}\text{-}^1\text{H}$ RDCs gives rise to broad, unresolved $^1\text{H}^{\text{N}}$ multiplets in the ^1H dimension of the 2D or 3D spectrum, thereby diminishing resolution and sensitivity, unless a very high level of deuteration is used in the protein [31]. The efficiency of gradient-enhanced HSQC schemes [11] is somewhat more sensitive to variations in the magnitude of the one-bond coupling, used for transferring magnetization, than the reverse INEPT transfer used in the original HSQC experiment. For a strongly aligned protein, such as ubiquitin in Pf1 phage, where the $^1J_{\text{NH}} + ^1D_{\text{NH}}$ value can vary by more than two-fold among different residues, we therefore prefer to use the single step, reverse INEPT HSQC to transfer magnetization back from ^{15}N to $^1\text{H}^{\text{N}}$.

The BASH-HSQC pulse sequence used in our measurement of RDCs in Pf1-aligned ubiquitin is shown in Fig. 1C. Suppression of the residual $^1\text{H}_2\text{O}$ signal is much less of a problem in heteronuclear NMR experiments than in homonuclear ^1H pulse schemes, such as 2D NOESY, and is easily accomplished by phase cycling of the 90_{ϕ_1} ^{15}N pulse in Fig. 1C, together with the receiver reference phase. It

is, however, important that the $^1\text{H}_2\text{O}$ signal in any individual scan remains sufficiently small that it does not overload the receiver. This latter requirement can be met by simply using z-gradient only pulses. So, whereas for the NOESY measurements we found it preferable to record the spectra on a probe equipped with three orthogonal gradients, HSQC spectra were recorded on a cryogenically cooled probehead, equipped with a z-gradient-only pulsed field gradient accessory.

Comparison of a small region of the ^1H - ^{15}N HSQC spectrum of ubiquitin in Pf1 highlights the gain in spectral resolution achieved by BASH decoupling (Fig. 3). It is important to note, however, that $^1\text{H}^{\text{N}}-^1\text{H}^{\text{N}}$ and $^1\text{H}^{\text{N}}-^1\text{H}^{\text{aromatic}}$ RDCs are not removed by BASH decoupling, and several amide resonances remain broader than in the corresponding isotropic spectrum (data not shown).

The HN(CO)CA extension of the HSQC experiment [32], recorded in the absence of ^1H decoupling in the $^{13}\text{C}^{\alpha}$ dimension, was used for measurement of $^1J_{\text{C}\alpha\text{H}\alpha} + ^1D_{\text{C}\alpha\text{H}\alpha}$ couplings in ubiquitin. The experiment was carried out twice, once with and once without BASH decoupling during $^1\text{H}^{\text{N}}$ detection, and the intensity ratio is compared in Fig. 4, with the noise level being identical in the two measurements. As can be seen, on average a significant improvement in signal to noise is obtained for most residues. However, a decrease is seen for residues where $^1\text{H}^{\text{N}}-^1\text{H}^{\text{aliphatic}}$ RDCs do not significantly impact the $^1\text{H}^{\text{N}}$ line width. In this case, the loss in signal that occurs during the BASH pulse pairs, with associated gradient pulses, results in faster apparent transverse relaxation in the directly detected dimension and more than offsets the line narrowing resulting from BASH decoupling. A decrease in sensitivity is also observed for residues whose amide protons are subject to rapid solvent exchange, as the reference HN(CO)CA spectrum was recorded without water presaturation.

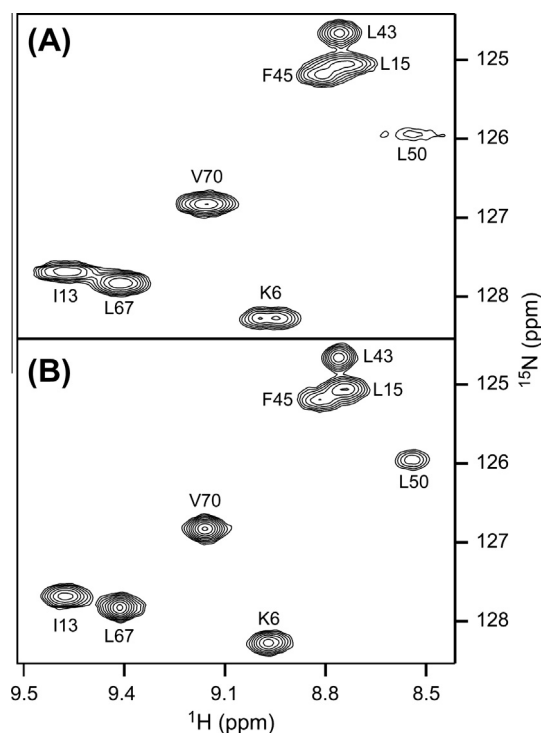


Fig. 3. Comparison of a small region of the BASH-decoupled and regular ^1H - ^{15}N HSQC spectrum of human ubiquitin (400 μM) in a liquid crystalline Pf1 suspension (13 mg/mL; 140 mM NaCl; pH 6.0, 25 $^{\circ}\text{C}$), recorded at 500 MHz with (A) the regular HSQC experiment, and (B) the same pulse scheme, but using BASH decoupling during t_2 acquisition (Fig. 1B).

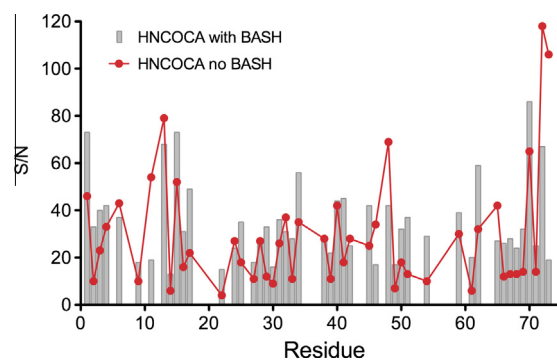


Fig. 4. Comparison of the average signal to noise ratio observed for the $^{13}\text{C}^{\alpha}-^1\text{H}^{\alpha}$ doublet components in a $^1\text{H}_2$ -coupled 3D HN(CO)CA experiment recorded with and without BASH decoupling during data acquisition on the same sample used for Fig. 3. The spectrum without BASH decoupling was recorded without water presaturation, the BASH-HN(CO)CA spectrum was recorded with weak water presaturation, causing some of the signals to be weaker in the BASH decoupled spectrum. The actual RDCs extracted from these two spectra are listed in Supplementary material Table S1.

A total of 47 $^1D_{\text{C}\alpha\text{H}\alpha}$ couplings could be extracted from the BASH-decoupled HN(CO)CA spectrum of ubiquitin in Pf1 (Supplementary information). With a Q factor of 15.5%, fitting of these couplings to the static solution NMR structure (PDB entry 1D3Z) [33] shows excellent agreement for the BASH-decoupled $^1D_{\text{C}\alpha\text{H}\alpha}$ values, and slightly lower agreement ($Q = 18.1\%$) for the values collected with the regular HN(CO)CA experiment.

3. Concluding remarks

We have demonstrated that band-selective homonuclear decoupling during the FID can result in considerable improvement of peptide and protein NMR spectra. The method and its possible applications are quite analogous to those of the homonuclear adiabatic decoupling scheme, proposed previously [15], but in our hands makes it less difficult to suppress the large water signal and its associated side-bands, and does not induce any offset-dependent shifts in peak positions resulting from the Bloch–Siegert effect.

Apparent broad-band decoupling in 2D NOESY and COSY spectra can also be accomplished by applying the decoupling scheme in only one of its dimensions, and then utilizing the intrinsic symmetry of such spectra in a post-acquisition covariance processing of the 2D spectrum [25]. This latter method is quite effective, in particular when t_1 noise ridges are not limiting spectral quality, but is restricted to spectra that are intrinsically symmetric, and therefore not applicable to the multitude of $^1\text{H}^{\text{N}}$ -detected heteronuclear 2D and 3D protein NMR experiments.

BASH decoupling also is applicable to ^{13}C -detected experiments of uniformly ^{13}C enriched proteins. For example, because of the large frequency separation between $^{13}\text{C}'$ and $^{13}\text{C}^{\alpha}$ resonances, BASH decoupling could be used instead of IPAP [34,35] to remove $^1J_{\text{C}\alpha\text{C}'}$ splittings in the detected $^{13}\text{C}'$ dimension.

Compared to the recently introduced ZS-decoupling scheme [7], BASH decoupling is less general in that only a subset of the scalar or dipolar interactions can be decoupled. On the other hand, BASH decoupling does not reduce the effective sample volume to a narrow, gradient-selected slice, and therefore observes the same number of spins studied in the regular non-decoupled experiments but with the added benefit of removal of $^3J_{\text{HH}}$ and $^1\text{H}-^1\text{H}$ RDC splittings. A slight decrease in intrinsic sensitivity relative to the regular experiment results from the small fraction of time during the FID where signal decays during the BASH pulse elements ($< \sim 10$ – 20% , decreasing S/N by 5– 10%), an effect that is usually more than offset

by the narrowing of the observed resonances resulting from the BASH decoupling. On Bruker spectrometers, interrupting the FID to apply pulses is not compatible with the use of their “digital receiver mode”, unless special processing software is used to undo the digital oversampling effect seen in the beginning of each interrupted signal acquisition block following each pair of selective and hard 180° pulses. Instead, the “analog mode” therefore must be used for signal detection. However, this analog detection on modern spectrometers such as the Bruker Avance-type systems is done automatically in an oversampling mode. Provided that the number of averaged, rapidly sampled data points used to generate one regular FID data point (“anavpt” parameter in Bruker pulse programs) is set to the highest possible value, use of this analog detection mode then does not appear to have a significant adverse effect on the signal to noise ratio compared to the digital receiver mode. Details on the pulse programming and parameter settings used for the experiments described here can be downloaded from <http://spin.niddk.nih.gov/bax/pp/>.

Acknowledgments

This work was funded by the Intramural Research Program of the National Institute of Diabetes and Digestive and Kidney Diseases, National Institutes of Health (NIH) and the Intramural AIDS-Targeted Antiviral Program of the Office of the Director, NIH.

Appendix A. Supplementary material

Supplementary data associated with this article can be found, in the online version, at <http://dx.doi.org/10.1016/j.jmr.2013.11.006>.

References

- [1] A. Bax, R. Freeman, Investigation of complex networks of spin–spin coupling by two-dimensional NMR, *J. Magn. Reson.* 44 (1981) 542–561.
- [2] F.J.M. van de Ven, M.E.P. Philippens, Optimization of constant-time evolution in multidimensional NMR experiments, *J. Magn. Reson.* 97 (1992) 637–644.
- [3] G.W. Vuister, A. Bax, Resolution enhancement and spectral editing of uniformly ^{13}C -enriched proteins by homonuclear broadband ^{13}C decoupling, *J. Magn. Reson.* 98 (1992) 428–435.
- [4] A. Bax, Broad-band homonuclear decoupling in heteronuclear shift correlation NMR spectroscopy, *J. Magn. Reson.* 53 (1983) 517–520.
- [5] K. Zangger, H. Sterk, Homonuclear broadband-decoupled NMR spectra, *J. Magn. Reson.* 124 (1997) 486–489.
- [6] N.H. Meyer, K. Zangger, Simplifying proton NMR spectra by instant homonuclear broadband decoupling, *Angew. Chem., Int. Ed.* 52 (2013) 7143–7146.
- [7] P. Sakhaii, B. Haase, W. Bermel, R. Kerssebaum, G.E. Wagner, K. Zangger, Broadband homodecoupled NMR spectroscopy with enhanced sensitivity, *J. Magn. Reson.* 233 (2013) 92–95.
- [8] R. Bruschweiler, C. Griesinger, O.W. Sørensen, R.R. Ernst, Combined use of hard and soft pulses for omega-1 decoupling in two-dimensional NMR spectroscopy, *J. Magn. Reson.* 78 (1988) 178–185.
- [9] J.R. Garbow, D.P. Weitekamp, A. Pines, Bilinear rotation decoupling of homonuclear scalar interactions, *Chem. Phys. Lett.* 93 (1982) 504–509.
- [10] G. Bodenhausen, D.J. Ruben, Natural abundance N-15 NMR by enhanced heteronuclear spectroscopy, *Chem. Phys. Lett.* 69 (1980) 185–189.
- [11] L.E. Kay, P. Keifer, T. Saarinen, Pure absorption gradient enhanced heteronuclear single quantum correlation spectroscopy with improved sensitivity, *J. Am. Chem. Soc.* 114 (1992) 10663–10665.
- [12] M. Ikura, L.E. Kay, A. Bax, A novel approach for sequential assignment of ^1H , ^{13}C , and ^{15}N spectra of larger proteins: heteronuclear triple-resonance three-dimensional NMR spectroscopy. Application to calmodulin, *Biochemistry* 29 (1990) 4659–4667.
- [13] G.T. Montelione, G. Wagner, Conformation-independent sequential NMR connections in isotope-enriched polypeptides by H-1-C-13-N-15 triple-resonance experiments, *J. Magn. Reson.* 87 (1990) 183–188.
- [14] M. Sattler, J. Schleucher, C. Griesinger, Heteronuclear multidimensional NMR experiments for the structure determination of proteins in solution employing pulsed field gradients, *Prog. NMR Spectrosc.* 34 (1999) 93–158.
- [15] C.W. Vander Kooi, E. Kupce, E.R.P. Zuiderweg, M. Pellecchia, Line narrowing in spectra of proteins dissolved in a dilute liquid crystalline phase by band-selective adiabatic decoupling: application to H-1(N)-N-15 residual dipolar coupling measurements, *J. Biomol. NMR* 15 (1999) 335–338.
- [16] A. Hammarström, G. Otting, Improved spectral resolution in ^1H NMR spectroscopy by homonuclear semiselective shaped pulse decoupling during acquisition, *J. Am. Chem. Soc.* 116 (1994).
- [17] A.S. Maltsev, A. Grishaev, A. Bax, Monomeric alpha-Synuclein binds Congo Red micelles in a disordered manner, *Biochemistry* 51 (2012) 631–642.
- [18] S.M. Gagne, S. Tsuda, M.X. Li, M. Chandra, L.B. Smillie, B.D. Sykes, Quantification of the calcium-induced secondary structural changes in the regulatory domain of troponin-C, *Protein Sci.* 3 (1994) 1961–1974.
- [19] A. Bax, Weak alignment offers new NMR opportunities to study protein structure and dynamics, *Protein Sci.* 12 (2003) 1–16.
- [20] M.R. Hansen, L. Mueller, A. Pardi, Tunable alignment of macromolecules by filamentous phage yields dipolar coupling interactions, *Nat. Struct. Biol.* 5 (1998) 1065–1074.
- [21] M. Zweckstetter, A. Bax, Characterization of molecular alignment in aqueous suspensions of Pf1 bacteriophage, *J. Biomol. NMR* 20 (2001) 365–377.
- [22] P. Plateau, M. Guéron, Exchangeable proton NMR without base-line distortion, using new strong-pulse sequences, *J. Am. Chem. Soc.* 104 (1982) 7310–7311.
- [23] H. Geen, R. Freeman, Band-selective radiofrequency pulses, *J. Magn. Reson.* 93 (1991) 93–141.
- [24] M.H. Levitt, R. Freeman, Composite pulse decoupling, *J. Magn. Reson.* 43 (1981) 502–507.
- [25] J.A. Aguilar, S. Faulkner, M. Nilsson, G.A. Morris, Pure shift ^1H NMR: a resolution of the resolution problem?, *Angew. Chem., Int. Ed.* 49 (2010) 3901–3903.
- [26] J. Graf, P.H. Nguyen, G. Stock, H. Schwalbe, Structure and dynamics of the homologous series of alanine peptides: a joint molecular dynamics/NMR study, *J. Am. Chem. Soc.* 129 (2007) 1179–1189.
- [27] M. Ottiger, F. Delaglio, A. Bax, Measurement of J and dipolar couplings from simplified two-dimensional NMR spectra, *J. Magn. Reson.* 131 (1998) 373–378.
- [28] J.R. Tolman, J.H. Prestegard, A quantitative J -correlation experiment for the accurate measurement of one-bond amide N-15-H-1 couplings in proteins, *J. Magn. Reson. Ser. B* 112 (1996) 245–252.
- [29] Y.X. Wang, J.L. Marquardt, P. Wingfield, S.J. Stahl, S. Lee-Huang, D. Torchia, A. Bax, Simultaneous measurement of H-1-N-15, H-1-C-13', and N-15-C-13' dipolar couplings in a perdeuterated 30 kDa protein dissolved in a dilute liquid crystalline phase, *J. Am. Chem. Soc.* 120 (1998) 7385–7386.
- [30] D.W. Yang, R.A. Venters, G.A. Mueller, W.Y. Choy, L.E. Kay, TROSY-based HNC0 pulse sequences for the measurement of (HN)-H- 1-N-15, N-15-(CO)-C-13, (HN)-H-1-(CO)-C-13, (CO)-C-13-C- 13(alpha) and (HN)-H-1-C-13(alpha) dipolar couplings in N-15, C-13, H-2-labeled proteins, *J. Biomol. NMR* 14 (1999) 333–343.
- [31] J.M. Ward, N.R. Skrynnikov, Very large residual dipolar couplings from deuterated ubiquitin, *J. Biomol. NMR* 54 (2012) 53–67.
- [32] M. Ikura, A. Bax, An efficient 3D NMR technique for correlating the proton and ^{15}N backbone amide resonances with the alpha-carbon of the preceding residue in uniformly $^{15}\text{N}/^{13}\text{C}$ enriched proteins, *J. Biomol. NMR* 1 (1991) 99–104.
- [33] G. Cornilescu, J.L. Marquardt, M. Ottiger, A. Bax, Validation of protein structure from anisotropic carbonyl chemical shifts in a dilute liquid crystalline phase, *J. Am. Chem. Soc.* 120 (1998) 6836–6837.
- [34] W. Bermel, I. Bertini, I.C. Felli, Y.M. Lee, C. Luchinat, R. Pierattelli, Protonless NMR experiments for sequence-specific assignment of backbone nuclei in unfolded proteins, *J. Am. Chem. Soc.* 128 (2006) 3918–3919.
- [35] E. Barbet-Massin, A.J. Pell, M.J. Knight, A.L. Webber, I.C. Felli, R. Pierattelli, L. Emsley, A. Lesage, G. Pintacuda, ^{13}C -detected through-bond correlation experiments for protein resonance assignment by ultra-fast MAS solid-state NMR, *ChemPhysChem* 14 (2013) 3131–3137.